

Double phase-conjugate mirror: analysis, demonstration, and applications

Shimon Weiss, Shmuel Sternklar, and Baruch Fischer

Department of Electrical Engineering, Technion-Israel Institute of Technology, Haifa 32000, Israel

Received February 26, 1986; accepted October 8, 1986

We report on the operation of the double phase-conjugate mirror (DPCM). Two inputs to opposite sides of a photorefractive barium titanate crystal, which may carry different spatial images, are shown to pump the same four-wave mixing process mutually and are self-refracted without any external or internal crystal surface. This results in the phase-conjugate reproduction of the two images simultaneously. This device is analyzed theoretically, and applications in image processing, interferometry, and rotation sensing are discussed. We also demonstrate the operation of a ring laser, using the DPCM, as well as a photorefractive resonator with two facing DPCM's that can support spatial information in its oscillations.

Various phase-conjugate mirrors (PCM's) and oscillators based on four-wave mixing (4WM) in photorefractive crystals have been proposed and demonstrated.¹⁻³ A double phase-conjugate mirror (DPCM), a 4WM device that through a transmission grating mechanism simultaneously phase conjugates two input beams impinging upon opposite sides of a photorefractive crystal, was not thought to be achievable.² We report here on the successful operation of the DPCM and theoretically analyze its properties. Applications for this device in image processing and interferometry are discussed.

The DPCM and experimental configuration are shown in Fig. 1. Two input beams, 2 and 4, are incident upon opposite surfaces of a photorefractive crystal. Because of 4WM in the crystal, these beams are self-bent into each other to produce output beams 3 and 1, which are phase conjugates of 4 and 2, respectively. The self-induced gratings are built up by beam couples 4, 1 and 2, 3. As a result of this mechanism, photons are transmitted from input beams 2 and 4 into beams 3 and 1, respectively; however, spatial information on beams 2 and 4 is reflected simultaneously from both sides of the crystal in a phase-conjugate form.

This device had been treated theoretically in both the degenerate and the nondegenerate cases.^{2,4} Its boundary conditions for the complex amplitudes A_i of the beams at the crystal faces are $A_4(z=0) = A_4(0)$, $A_2(z=l) = A_2(l)$, and $A_1(0) = A_3(l) = 0$. We use the notation and results summarized in Ref. 2 and show that all quantities can be expressed by the input-beam ratio $q = I_4(0)/I_2(l)$, where $I_i(z) = |A_i(z)|^2$. The conserved normalized power-density flux Δ , defined by $\Delta = [(I_2 + I_3) - (I_1 + I_4)]/I_0$, where $I_0 = \sum I_i$, is given here by $\Delta = (1 - q)/(1 + q)$. The complex amplitude transmissivities are the same in both directions, i.e., $A_3(0)/A_2(l) = A_1(0)/A_4(0)$. An expression for the symmetric intensity transmission, $T = I_3(0)/I_2(l) = I_1(l)/I_4(0)$, is given by

$$T = \frac{a^2[q^{-1/2} + q^{1/2}]^2 - [q^{-1/2} - q^{1/2}]^2}{4}, \quad (1)$$

where a is related to the coupling coefficient γ by

$$\tanh\left(-\frac{\gamma l}{2} a\right) = a. \quad (2)$$

We find for the reflectivities of the device $R_1 = I_3(0)/I_4(0)$ and $R_2 = I_1(l)/I_2(l)$ that

$$R_1 = T/q, \quad R_2 = Tq. \quad (3)$$

Equation (2) gives the lowest threshold possible for γl , $|(\gamma l)_t| = 2$. From Eq. (1) we see that for $q = 1$ the transmission is maximum and equal to a^2 and derive the range of q for oscillation to be

$$\frac{1-a}{1+a} < q < \frac{1+a}{1-a}. \quad (4)$$

Above the threshold $[|(\gamma l)_t| = 2]$, the value of a is close to its upper limit, i.e., $a \approx 1$, so that it is useful to express the device's transmissions and reflectivities at this limit:

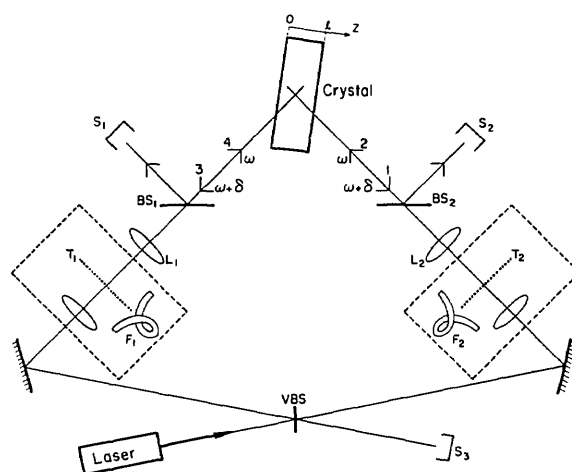


Fig. 1. Schematic of the experimental setup for the DPCM: VBS, variable beam splitter; BS's, beam splitters; T's, transparencies; L's, lenses; F's, optical fibers; S's, screens. Possible frequency nondegeneracy in the beams is denoted by δ . The laser's output frequency is ω (see Ref. 4).

$$T \rightarrow 1, \quad R_{1,2} \rightarrow q^{-1}. \quad (5)$$

However, losses in the crystal will decrease the transmission and reflection appreciably.

We have observed that when two light beams are directed into a photorefractive BaTiO₃ crystal in a DPCM configuration, loosely focusing and guiding the beams to maximum spatial overlap in the crystal permits efficient 4WM to occur. This dynamic process, pumped simultaneously by the two inputs, builds up two oscillation beams with clearly defined wave vectors counterpropagating with respect to the inputs. We checked that each reflection originated from the other pump and not by any self-pumped phase conjugation or two-beam coupling. This was done by examining the light channel in the crystal during operation. Blocking either of the inputs after oscillation built up did not cause an instantaneous erasure of its counterpropagating phase-conjugate output, which continued to appear with slight decay during the blocking.⁵ An interferometric check verified this mechanism.

To test the fidelity of these phase-conjugate beams, we set up the configuration shown in Fig. 1. The 488-nm-line output of an argon-ion laser without an étalon having extraordinary polarization was split by a variable beam splitter (VBS) into two input beams, 4 and 2. Beam 4 picked up pictorial information T_1 on its way to the $z = 0$ face of a photorefractive BaTiO₃ crystal, and beam 2 carried information T_2 into the $z = l$ face of the same crystal. The crystal dimensions were 7 mm \times 6 mm \times 3 mm. The geometry of the beams in the crystal was similar to that in earlier papers; see Refs. 2 and 6. The c axis of the crystal along the 7-mm side was parallel to the z direction in Fig. 1. The angle between input beams 4 and 2 inside the crystal was approximately 173°. The VBS and lenses, L_1 and L_2 , both with $f = 150$ mm, were used to ensure optimum intensity ratio q and overlap of beams 2 and 4 in the crystal (as explained earlier), which were loosely focused to a diameter of 1 mm. Phase-conjugate beams 3 and 1 built up within the crystal and emerged with the full pictorial information of T_1 and T_2 , respectively. These output images, seen simultaneously at screens S_1 and S_2 , are shown in Fig. 2. The absence of significant cross talk observed between the image-bearing input beams is discussed in detail in a future publication.

When the two input arms from the VBS to the crystal were of equal length, the two DPCM outputs were quite sensitive to slight vibrations. We attribute this to the presence of reflection gratings⁶ written by beams 2 and 4 that were in coherence. We lengthened one input arm so that beams 2 and 4 were mutually incoherent. This resulted in stable outputs that were completely insensitive to table vibrations. The DPCM can operate with mutually incoherent inputs since the transmission grating is written by beam pairs 4, 1 and 2, 3. The contribution to this grating from both beam pairs can still spatially overlap.⁷ The production of counterpropagating phase-conjugate pairs² results in maximum spatial overlap and hence maximum gain in the crystal.

We also point out that the DPCM is actually a new

passive phase-conjugate mirror (PPCM). Spatial information between the laser and the VBS of Fig. 1, without T_1 and T_2 , will be phase conjugated by the DPCM.

The DPCM can be used to construct a Sagnac interferometer with optical fibers that is useful for rotation sensing. This is represented in Fig. 1 by the two fiber links F_1 and F_2 (replacing the slides and related optics), which may be multimode because of the phase-conjugating nature of the DPCM. We note that gyroscopes incorporating PCM's were suggested in the past. These include a conventional gyroscope with an externally pumped PCM⁸ and another based on a self-detuning mechanism in the ring PPCM.⁹ As in regular Sagnac interferometers, the use of a 3-dB beam splitter in place of the VBS will cause destructive interference at screen S_3 in the absence of nonreciprocal phase in the ring. This also suggests its use as an image subtractor for two input images T_1 and T_2 , since at S_3 there will appear $T_2 - T_1$.

We operated a ring laser using the DPCM, as proposed and analyzed in Ref. 2 and shown in Fig. 14 of that reference. An argon-ion gain cavity was used, with two VBS's gradually rotated to maximum transmission after serving initially as the laser's end mirrors. Lasing built up as counterpropagating oscilla-

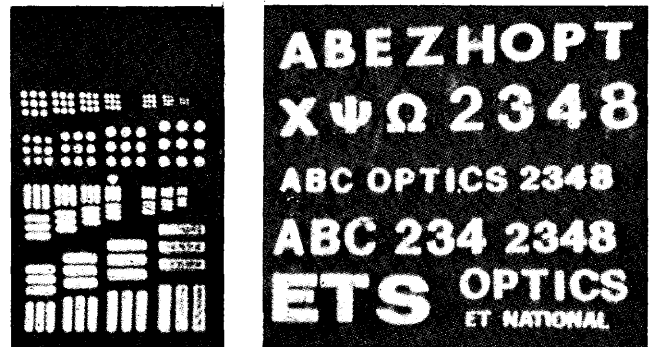


Fig. 2. Output beams 3 and 1 of the DPCM seen simultaneously at S_1 and S_2 (from left to right). The pictures display a resolution of better than 5 lines/mm.

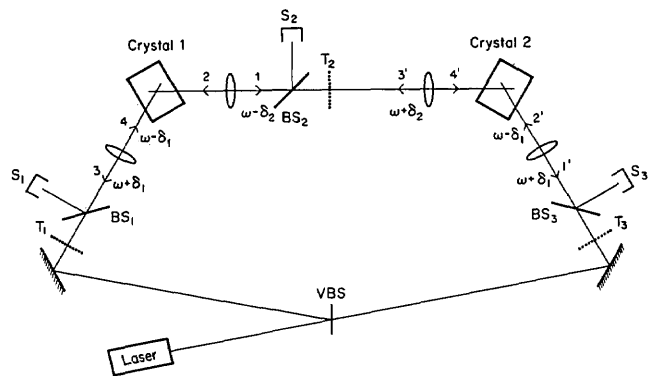


Fig. 3. Schematic of the experimental setup for oscillator by two facing DPCM's. Symbols are as in Fig. 1. Frequency degeneracy is denoted by δ_1 and δ_2 (see Ref. 4).

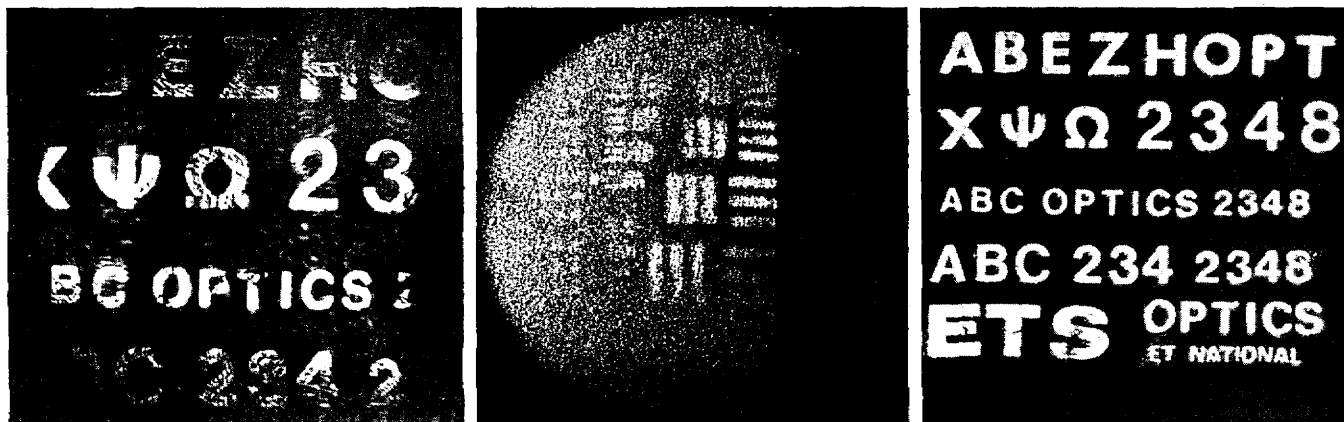


Fig. 4. Oscillation beams 3, 1, and 1' of Fig. 4 seen simultaneously at screens S_1 , S_2 , and S_3 (from left to right).

tion beams in the ring cavity, which contained the BaTiO_3 crystal as the DPCM. We note that this configuration can act as a laser gyro, with multimode fibers in the ring.

Finally, we formed a photorefractive oscillation between two facing DPCM's, as is shown in Fig. 3. Beam 4 with information T_1 and beam 2' with information T_3 entered photorefractive BaTiO_3 crystals 1 and 2, respectively. Oscillation beams 1(4') and 3'(2) supporting information T_2 built up between the crystals, which were now acting as DPCM's for their respective inputs. These beams as well as outputs 3 and 1' carried the spatial information for the three different inputs. The images, seen simultaneously at screens S_1 , S_2 , and S_3 for oscillation beams 3, 1, and 1', respectively, are shown in Fig. 4. We recently demonstrated another photorefractive oscillator, the two-cascaded PPCM resonator.¹⁰ This oscillator was shown to support spatial information in an oscillation between two semilinear PPCM's placed in tandem. Here we see that the two facing DPCM's can support three different images simultaneously in their oscillations without significant cross talk, as in the DPCM discussed above. These configurations are suitable for the iterative buildup of spatial information, such as in associative memories¹¹ and implementations of filtering,¹² or image reconstruction algorithms such as phase retrieval.¹³ The DPCM may be useful in an optical associative memory implementation, since a theoretical and experimental analysis, to be published elsewhere, shows that it can display tunable thresholding and reflection gain.

We have demonstrated the operation of the DPCM for two different input images, theoretically analyzed and shown to be a new PPCM configuration. It can be used to construct a Sagnac interferometer and a ring laser with applications in rotation sensing and image subtraction. Both can incorporate multimode fibers in their rings. We concluded with a demonstration of a photorefractive oscillator with two facing DPCM's

that can support different images in three regions of the resonator, which is useful for the implementation of iterative image processing algorithms.

This research was supported by the Technion VPR-Henri Gutwirth fund for the promotion of research.

References

1. J. Feinberg and R. W. Hellwarth, *Opt. Lett.* **5**, 519 (1980).
2. M. Cronin-Golomb, B. Fischer, J. O. White, and A. Yariv, *IEEE J. Quantum Electron.* **QE-20**, 12 (1984).
3. K. R. MacDonald and J. Feinberg, *J. Opt. Soc. Am.* **73**, 548 (1983).
4. B. Fischer, *Opt. Lett.* **11**, 236 (1986).
5. This ruled out a possible backscattering mechanism such as that discussed by T. Y. Chang and R. W. Hellwarth, *Opt. Lett.* **10**, 408 (1985).
6. M. Cronin-Golomb, J. Paslaski, and A. Yariv, *Appl. Phys. Lett.* **47**, 1131 (1985).
7. The DPCM can operate even with inputs derived from separate lasers, with the maximum allowable difference in wavelength between the two lasers dictated by the Bragg selectivity of the thick gratings. This is demonstrated in a subsequent work by S. Sternklar, S. Weiss, M. Segev, and B. Fischer, *Opt. Lett.* **11**, 528 (1986).
8. Ph. Graindorge, H. J. Arditty, M. Papuchon, J. P. Huignard, and Ch. Bordé, in *Fiber Optic Rotation Sensors and Related Technologies*, S. Ezekiel and H. J. Arditty, eds. (Springer-Verlag, New York, 1982), pp. 368-374.
9. B. Fischer and S. Sternklar, *Appl. Phys. Lett.* **47**, 1 (1985).
10. B. Fischer, S. Sternklar, and S. Weiss, *Appl. Phys. Lett.* **48**, 1567 (1986).
11. D. Z. Anderson, *Opt. Lett.* **11**, (1986); B. H. Soffer, G. J. Dunning, Y. Owechko, and E. Marom, *Opt. Lett.* **11**, 118 (1986); A. Yariv and S. K. Kwong, *Opt. Lett.* **11**, 186 (1986).
12. O. Ikeda, T. Sato, and H. Kojima, *J. Opt. Soc. Am. A* **2**, 1863 (1985); **3**, 645 (1986).
13. R. H. Boucher, *Proc. Soc. Photo-Opt. Instrum. Eng.* **231**, 130 (1980).